and the results will be reported in the future.

The reaction of $CrTPPS(H_2O)_2^{3-}$ with Im has been studied at 15, 25, and 35 °C in aqueous solution over the accessible pH range. The values of the equilibrium and rate constants and activation parameters are reported. The porphyrin ligand labilizes the Cr(III) to ligation, with the trans OH^- ligand labilizing even more. There are no clear trends in the values of the activation parameters and the labilization other than, in general, the values of ΔH^* are about 16 kcal mol^{-1}.

Acknowledgment. This research was supported by the Robert A. Welch Foundation, Houston, TX, and an East Texas State University Faculty Research Grant.

Registry No. $CrTPP(H_2O)_2^{3-}$, 33339-70-7; Im, 288-32-4.

Contribution from the School of Chemical Sciences,
University of Illinois at Urbana-Champaign, Urbana, Illinois 61801

Tetrathiometalate Complexes of Rhodium, Iridium, Palladium, and Platinum. Structures of $[(C_5Me_5)RhCl]_2WS_4$ and $[(C_3H_5)Pd]_2WS_4$

Kevin E. Howard, Thomas B. Rauchfuss,* and Scott R. Wilson

Received March 23, 1988

Synthetic routes to tetrathiometalate complexes of rhodium, iridium, palladium, and platinum are described. Acetonitrile solutions of WS_4^{2-} reacted with $[Rh(diene)Cl]_2$ (where diene = 1,5-cyclooctadiene (COD) or norbornadiene (NBD)), $[Ir(COD)Cl]_2$, $[(\eta^5\text{-}C_5Me_5)RhCl_2]_2$, and $[Pd(allyl)Cl]_2$ to give good yields of μ-WS_4 complexes $[Rh(diene)]_2WS_4$, $[Ir(COD)]_2WS_4$, $[(\eta^5\text{-}C_5Me_5)RhCl]_2WS_4$, and $[(allyl)Pd]_2WS_4$, respectively. $(COD)PtCl_2$ reacted with MS_4^{2-} to give $(COD)PtMS_4$, M = Mo, W. The latter complexes react further with PPh_3 or WS_4^{2-} to give $(PPh_3)_2PtMS_4$ and $Pt(WS_4)_2^{2-}$, respectively. $[Rh(COD)]_2WS_4$ reacted with *t*-BuNC to give $[Rh(t\text{-}BuNC)_2]_2WS_4$. $RhCl_3\cdot 3H_2O$ and $IrCl_3\cdot H_2O$ react with WS_4^{2-} to give the octahedral complexes $M(WS_4)_3^{3-}$ isolated as their Et_4N^+ salts. The ^{183}W NMR spectrum of $(Et_4N)_3[Rh(WS_4)_3]$ showed a doublet with $J(^{183}W,^{103}Rh) = 4.8$ Hz. Thermal gravimetric analyses of $[Rh(COD)]_2WS_4$ and $(COD)PtWS_4$ indicate that loss of organic coligands and stoichiometric amounts of sulfur occur at moderate temperatures. The compound $[(\eta^5\text{-}C_5Me_5)RhCl]_2WS_4\cdot CHCl_3$ crystallizes in the orthorhombic space group $P2_12_12_1$ with $a = 13.179$ (2) Å, $b = 28.725$ (7) Å, $c = 8.258$ (2) Å, $V = 3126$ (2) Å^3, and $Z = 4$ and was refined to $R = 0.052$ and $R_w = 0.059$. The compound $[(\eta^3\text{-}C_3H_5)Pd]_2WS_4$ crystallizes in the monoclinic space group $P2_1/c$ with $a = 9.230$ (4) Å, $b = 9.994$ (5) Å, $c = 14.780$ (7) Å, $\beta = 103.54$ (4)°, $V = 1325$ (1) Å^3, and $Z = 4$ and was refined to $R = 0.066$ and $R_w = 0.079$.

Introduction

In this report we describe the synthesis of tetrathiometalate complexes of rhodium, iridium, palladium, and platinum. At the inception of this investigation[1] little was known about the thiometalate complexes of the platinum metals[2] and no thiometalate complexes of rhodium or iridium had been reported.[3] Given the well-established affinity of platinum for sulfur ligands,[4] this aspect of coordination chemistry seemed likely to be very rich. Two classes of compounds were prepared, square-planar d^8 complexes and octahedral d^6 complexes. Thiometalate complexes of d^8 ions have been known for some time, viz. $M(M'S_4)_2^{3-}$ (where M = Co; M′ = Mo, W)[5,6] and $M(M'S_4)_2^{2-}$ (where M = Ni, Pd, Pt; M′ = Mo, W).[2] Octahedral d^6 thiometalate complexes are much less common.[7,8] We describe the first examples of tris(tetrathiometalate) complexes in the form of $M(WS_4)_3^{3-}$, where M = Rh, Ir.

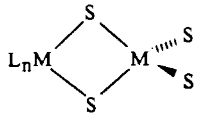

A

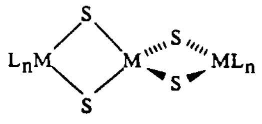

B

Thiometalates commonly function as either terminal (A) or bridging (B) bidentate ligands. In type A complexes, the MS_4 metallo ligand can be viewed as a pseudohalide, 2e chelating agent. It is clear, however, that tetrathiometalates are not simple dithio chelates: whereas 1,1-dithiolenes stabilize metals in high formal oxidation states,[9] MoS_4^{2-} and WS_4^{2-} stabilize metals in their lower oxidation states.[10] In the bridging mode (B), each half of the MS_4 group resembles a dithio acid or 3e ligand. Recent work from this laboratory has shown that such bridging tetrathiometalates can promote strong electronic communication between the terminal metal sites.[11] For example carbonylation of $[CpRu(PPh_3)]_2WS_4$ proceeds only to the monocarbonyl stage despite the fact that the $CpRu(PPh_3)$ centers are equivalent and 5.65 Å apart (eq 1). Intermetallic electronic coupling is also indicated for the one-dimensional semiconductor NH_4CuMoS_4.[12] Recently complexes have been described in which metal atoms bridge adjacent edges of the thiometalate tetrahedron, such as

---

(1) Howard, K. E.; Rauchfuss, T. B.; Rheingold, A. L. *J. Am. Chem. Soc.* **1986**, *108*, 297.

(2) (a) Callahan, K. P.; Cichon, E. J. *Inorg. Chem.* **1981**, *20*, 1941. (b) Siedle, A. R.; Hubbard, C. R.; Mighell, A. D.; Doherty, R. M.; Stewart, J. M. *Inorg. Chim. Acta* **1980**, *38*, 197. (c) Callahan, K. P.; Piliero, P. A. *Inorg. Chem.* **1980**, *19*, 2619. (d) Callahan, K. P.; Piliero, P. A. *J. Chem. Soc., Chem. Commun.* **1979**, 13. (e) Müller, A.; Heinsen, H.-H.; Vandrish, G. *Inorg. Chem.* **1974**, *13*, 1001. (f) Müller, A.; Diemann, E. *J. Chem. Soc., Chem. Commun.* **1971**, 65.

(3) (a) Müller, A.; Diemann, E.; Jostes, R.; Bögge, H. *Angew. Chem., Int. Ed. Engl.* **1981**, *10*, 934. (b) Coucouvanis, D. *Acc. Chem. Res.* **1981**, *14*, 201. (c) Holm, R. H. *Chem. Soc. Rev.* **1981**, *10*, 455.

(4) See, for example: Roundhill, D. M. In *Comprehensive Coordination Chemistry*; Wilkinson, G., Gillard, R. D., McCleverty, J. A., Eds.; Pergamon: Oxford, England, 1987; Vol. 5, Chapter 52, p 471. Hartley, F. R. *The Chemistry of Platinum and Palladium*; Wiley: New York, 1973; Chapter 8 and references therein.

(5) Pan, W.-H.; Johnston, D. C.; McKenna, S. T.; Chianelli, R. R.; Halbert, T. R.; Hutchings, L. L.; Stiefel, E. I. *Inorg. Chim. Acta* **1985**, *97*, L17.

(6) Müller, A.; Hellmann, W.; Schneider, J.; Schimanski, U.; Demmer, U.; Trautwein, A.; Bender, U. *Inorg. Chim. Acta* **1982**, *65*, L41.

(7) Tanaka, K.; Morimoto, M.; Tanaka, T. *Inorg. Chim. Acta* **1981**, *56*, L61.

(8) Stremple, P.; Baenziger, N. C.; Coucouvanis, D. *J. Am. Chem. Soc.* **1981**, *103*, 4601.

(9) Coucouvanis, D. *Prog. Inorg. Chem.* **1970**, *11*, 233; **1979**, *26*, 301.

(10) Bowmaker, G. A.; Boyd, P. D. W.; Sorrenson, R. J.; Reed, C. A.; McDonald, J. W. *Inorg. Chem.* **1987**, *26*, 3.

(11) Howard, K. E.; Rauchfuss, T. B.; Wilson, S. R. *Inorg. Chem.* **1988**, *27*, 1710.

(12) Binnie, W. P.; Redman, M. J.; Mallio, W. J. *Inorg. Chem.* **1970**, *9*, 1449. Redman, M. J. *Inorg. Synth.* **1973**, *14*, 95.

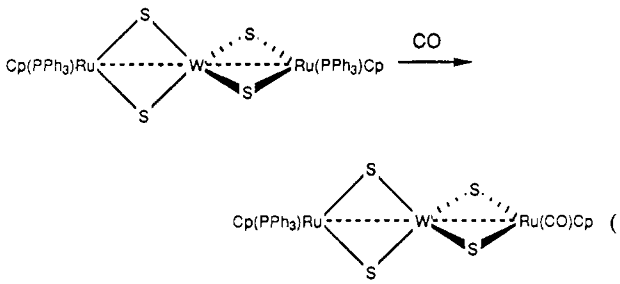

(1)

(Ph$_4$P)$_2$[(CuCNS)$_4$WS$_4$][13] and related gold complexes.[14]

Our syntheses entail the metathetical reactions of platinum metal chlorides and the tetrathiometalates MoS$_4^{2-}$ and WS$_4^{2-}$. As such, our methods represent an extension of the original work of Müller and co-workers.[3a] Organometallic complexes were found to be particularly amenable to this strategy. Because of the lability of the organic coligands, the new thiometalate complexes undergo further reactions. Perhaps more significantly, electrically neutral thiometalates (most known thiometalate complexes are anionic) with labile organic ligands appear to be promising precursors to new inorganic solids.

Results and Discussion

Most of the studies described in this paper concern complexes of tetrathiotungstate. Organic salts of WS$_4^{2-}$ appear to be more resistant to hydrolysis and oxidation than the corresponding tetrathiomolybdates. An important synthetic detail is that dichloromethane solutions of (Ph$_4$P)$_2$WS$_4$ are stable whereas the molybdate is not. In those cases where we have prepared the corresponding tetrathiomolybdate derivatives,[11] spectroscopic evidence indicates that they are structurally analogous to the tungsten compounds.

Investigations on neutral clusters derived from WS$_4^{2-}$ (and MoS$_4^{2-}$) are often limited by solubility considerations. It is rare for neutral *inorganic* complexes to exhibit good solubility. Often large, alkylated organic coligands were required for solubility sufficient for 200-MHz ^{1}H NMR characterization. Syntheses were often modeled after related metathetical reactions involving 1,1-dithio anions, e.g. Et$_2$NCS$_2^-$.[9,15] It was found that (μ-Cl)$_2$ complexes reliably served as precursors to μ-MS$_4$ derivatives (eq 2).

$$(\mathrm{L}_n\mathrm{M})_2(\mu\text{-Cl})_2 + \mathrm{MS}_4^{2-} \rightarrow (\mathrm{L}_n\mathrm{M})_2(\mu\text{-MS}_4) + 2\mathrm{Cl}^- \quad (2)$$

[Rh(NBD)]$_2$WS$_4$ (1). In close analogy to our recent preparation of [Rh(COD)]$_2$WS$_4$,[1] the reaction of acetonitrile solutions of [Rh(NBD)Cl]$_2$[16] (where NBD = norbornadiene) and (Ph$_4$P)$_2$WS$_4$ resulted in the immediate precipitation of an orange solid. Recrystallization gave a 75% yield of red-orange crystals of [Rh(NBD)]$_2$WS$_4$. This complex is somewhat more soluble in dichloromethane and chloroform than the corresponding cyclooctadiene derivative.[1] As in the case of the COD derivative, **1** displayed no hydrogenation activity toward 1-hexene even at 850 psig of H$_2$.

[Rh(*t*-BuNC)$_2$]$_2$WS$_4$ (2). In our original report[1] we described how the diene ligands in [Rh(COD)]$_2$WS$_4$ undergo substitution by phosphines and a combination of triphenylphosphine and CO. Carbonylation of [Rh(COD)]$_2$WS$_4$ led to decomposition, indicating that [Rh(CO)$_2$]$_2$WS$_4$ is not stable, possibly due to the competing acceptor properties of CO and μ-WS$_4$ moieties. Using *t*-BuNC, an electron-rich surrogate of CO, we were able to displace the cyclooctadiene ligands, giving [Rh(*t*-BuNC)$_2$]$_2$WS$_4$, isolated in high yield as stable red crystals (eq 3). The ^{1}H NMR spectrum

$$[\mathrm{Rh(COD)}]_2\mathrm{WS}_4 + 4\ t\text{-BuNC} \rightarrow [\mathrm{Rh}(t\text{-BuNC})_2]_2\mathrm{WS}_4 + 2\mathrm{COD} \quad (3)$$

of **2** consists of a singlet at 1.61 ppm, shifted 0.16 ppm downfield from free *t*-BuNC. The IR spectrum of a CH$_2$Cl$_2$ solution of **2** shows a strong ν_{NC} band at 2164 cm^{-1} whereas a CH$_2$Cl$_2$ solution of *t*-BuNC exhibits a band at 2140 cm^{-1}. The latter data indicate that the isocyanide is functioning as a net *donor* ligand. The complex [RhCl(*t*-BuNC)$_2$]$_2$, for comparison, exhibits a ν_{NC} band at 2230 cm^{-1} in its IR spectrum (Nujol).[17]

[Ir(COD)]$_2$WS$_4$ (3). In a further extension of our [Rh(COD)]$_2$WS$_4$ synthesis,[1] we prepared the corresponding iridium species, [Ir(COD)]$_2$WS$_4$, in good yield. This air-stable, red-brown microcrystalline compound is soluble in CH$_2$Cl$_2$ and CHCl$_3$. As with the rhodium analogue, **3** reacts with PPh$_3$ and it likely has an extensive substitution chemistry. The infrared spectrum of this complex exhibits a ν_{WS} band at 464 cm^{-1}, which is essentially the same as that observed for the rhodium analogue (466 cm^{-1}). The ^{1}H NMR spectra of the rhodium and iridium compounds are very similar.

[(η^5-C$_5$Me$_5$)RhCl]$_2$WS$_4$ (4). Acetonitrile solutions of (C$_5$Me$_5$)$_2$Rh$_2$Cl$_4$[18] and (Ph$_4$P)$_2$WS$_4$ reacted rapidly to give red microcrystalline [(C$_5$Me$_5$)RhCl]$_2$WS$_4$. This air-stable red complex exhibits a singlet in its ^{1}H NMR spectrum at 1.97 ppm. The presence of chloride ligands in this highly soluble compound suggested that reduction in the presence of small-molecule substrates might lead to new low-valent systems. However, reduction with Na/Hg, Zn, Zn/Hg, or Mg in the presence of olefins, acetylenes, H$_2$, CO, and N$_2$ gave no tractable products. Unlike isoelectronic [CpRuL]$_2$WS$_4$ compounds, which undergo well-defined one-electron oxidations,[11] acetonitrile solutions of **4** exhibit no reversible electrochemistry in the range of +1.2 to −1.2 V (vs Ag/AgCl).

[(allyl)Pd]$_2$WS$_4$ (5). This compound was prepared in good yield from the reaction of (Ph$_4$P)$_2$WS$_4$ and (all)$_2$Pd$_2$Cl$_2$. The ^{1}H NMR spectrum of **5** shows a septet and two doublets, consistent with η^3-allyl ligands.[19] An unusual feature of this compound is its very low organic content of 12.28% carbon and its very high density, calculated to be 3.042 g cm^{-3} on the basis of the crystallographic results (vide infra). The good solubility of **5** is surprising in view of its low organic content. The ν_{WS} band observed at 454 cm^{-1} is similar to that for other μ-MS$_4$ complexes (Figure 1).

(COD)PtMoS$_4$ (6) and (COD)PtWS$_4$ (7). The reaction of colorless acetonitrile solutions of PtCl$_2$(COD)[20] with (PPh$_4$)$_2$MS$_4$ (where M = Mo (**6**) or W (**7**)) gave red-brown (Mo) or yellow (W) precipitates. These neutral compounds are insoluble in common organic solvents but were obtained in analytically pure form. The infrared spectra of **6** and **7** feature two moderately intense bands at 506 and 468 cm^{-1} (Mo) and at 499 and 453 cm^{-1} (W) assigned to ν_{MS}(terminal) and ν_{MS}(bridging), respectively (Figure 1). Dichloromethane suspensions of MS$_4$Pt(COD) react slowly with an excess of triphenylphosphine to give (PPh$_3$)$_2$PtMS$_4$ (eq 4). These and similar phosphine complexes are moderately

$$(\mathrm{COD})\mathrm{PtWS}_4 + 2\mathrm{PPh}_3 \rightarrow (\mathrm{PPh}_3)_2\mathrm{PtMS}_4 + \mathrm{COD} \quad (4)$$

soluble and have been previously reported by Siedle, Potvin, and their co-workers.[21] The ^{31}P NMR spectra of these compounds each consisted of a singlet flanked by ^{195}Pt satellites with $|J(^{31}\mathrm{P}, ^{195}\mathrm{Pt})|$ = 3434 Hz (M = Mo) and $|J(^{31}\mathrm{P}, ^{195}\mathrm{Pt})|$ = 3484 Hz (M = W).

---

(13) (a) Potvin, C.; Manoli, J.-M.; Sêcheresse, F.; Marzak, S. *Inorg. Chem.* **1987**, *26*, 4370. (b) Manoli, J.-M.; Potvin, C.; Sêcheresse, F.; Marzak, S. *J. Chem. Soc., Chem. Commun.* **1986**, 1557. For additional examples see: (c) Müller, A.; Hellmann, W.; Bögge, H.; Jostes, R.; Römer, M.; Schimanski, U. *Angew. Chem., Int. Ed. Engl.* **1982**, *21*, 860. (d) Stalick, J. K.; Siedle, A. R.; Mighell, A. D.; Hubbard, C. R. *J. Am. Chem. Soc.* **1979**, *101*, 2832. (e) Sêcheresse, F.; Salis, M.; Potvin, C.; Manoli, J.-M. *Inorg. Chim. Acta* **1986**, *114*, L19.

(14) Charnock, J. M.; Bristow, S.; Nicholson, J. R.; Garner, C. D.; Clegg, W. *J. Chem. Soc., Dalton Trans.* **1987**, 303.

(15) Callahan, K. P.; Cichon, E. J. *Inorg. Chem.* **1981**, *20*, 1941. Burns, R. P.; McCullough, F. P.; McAuliffe, C. A. *Adv. Inorg. Chem. Radiochem.* **1980**, *23*, 211.

(16) Abel, E. W.; Bennett, M. A.; Wilkinson, G. *J. Chem. Soc.* **1959**, 3178.

(17) Branson, P. R.; Green, M. *J. Chem. Soc., Dalton Trans.* **1972**, 1303.

(18) Kang, J. W.; Moseley, K.; Maitlis, P. M. *J. Am. Chem. Soc.* **1969**, *91*, 5970.

(19) Dehm, H. C.; Chien, J. C. W. *J. Am. Chem. Soc.* **1960**, *82*, 4429.

(20) Drew, D.; Doyle, J. R. *Inorg. Synth.* **1972**, *13*, 48.

(21) Siedle, A. R.; Hubbard, C. R.; Mighell, A. D.; Doherty, R. M.; Stewart, J. M. *Inorg. Chim. Acta* **1980**, *38*, 197. Potvin, C.; Manoli, J.-M.; Sêcheresse, F.; Marzak, S. *Inorg. Chim. Acta* **1987**, *134*, 9.

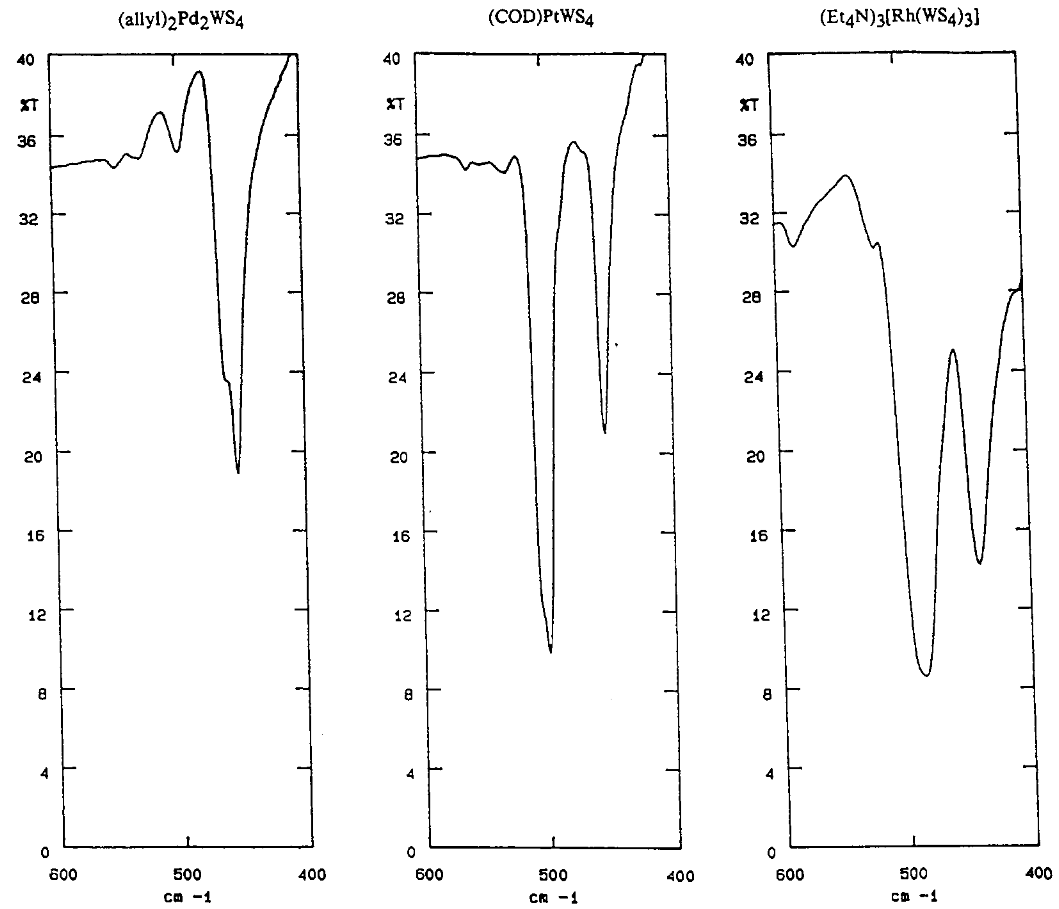

Figure 1. IR spectra in the ν_{WS} region illustrating the bands diagnostic for μ-WS_4 and terminal WS_4 ligation modes.

Treatment of an acetonitrile suspension of (COD)$PtWS_4$ with 1 equiv of WS_4^{2-} gave a reddish orange solution, the UV–visible spectrum of which matched that for $Pt(WS_4)_2^{2-}$ (eq 5).[2]

$$(COD)PtWS_4 + WS_4^{2-} \rightarrow Pt(WS_4)_2^{2-} + COD \qquad (5)$$

$(Et_4N)_3[M(WS_4)_3]$ (M = Rh (8), Ir (9)). The tris(tetrathiometalate) complexes $(Et_4N)_3[M(WS_4)_3]$ (M = Rh, Ir) were prepared by the direct reaction of alcohol solutions of hydrated trichlorides of rhodium and iridium with 3 equiv of $(Et_4N)_2WS_4$. After several days at room temperature, these solutions gave somewhat powdery precipitates that could be recrystallized. Despite repeated attempts, we were unable to obtain X-ray-quality single crystals of these compounds. Both compounds exhibit two ν_{WS} bands in their infrared spectra, one for bridging and one for terminal W–S vibrations (Figure 1). $(Et_4N)_3[Rh(WS_4)_3]$ was shown to be a 3:1 electrolyte by comparing its solution conductivity to that of Et_4NCl and $(Et_4N)_2WS_4$. The rhodium derivative was also characterized by ^{183}W NMR spectroscopy (Figure 2); the spectrum consists of a doublet at +2948 ppm downfield from Na_2WO_4 with $J(^{183}W, ^{103}Rh) = 4.8$ Hz (^{103}Rh: $I = {}^1/_2$, 100% natural abundance). The ^{183}W NMR resonance for $(NH_4)_2WS_4$ is reported as +3769 ppm while a shift of +2641 ppm was observed for $(Pr^n{}_4N)_2[(NCCu)_2WS_4]$.[22] Our spectroscopic data indicate that compounds 8 and 9 feature octahedral trivalent metals bound to three bidentate WS_4^{2-} ligands:[23]

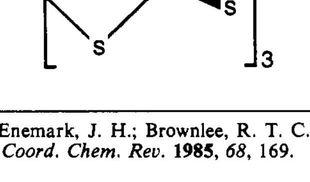

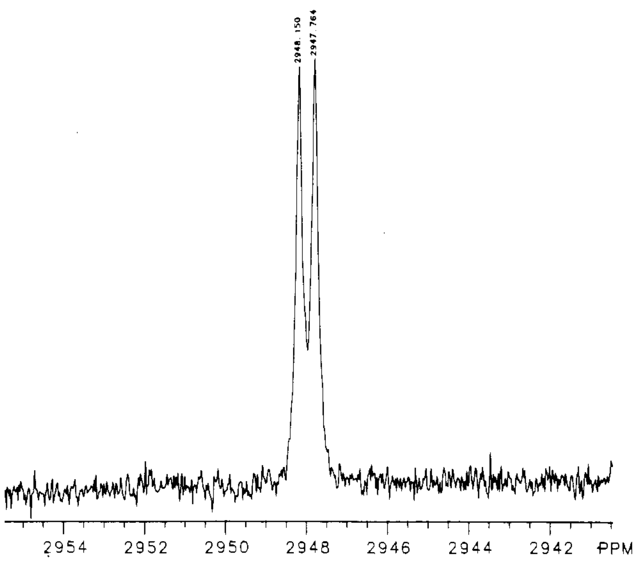

Figure 2. ^{183}W NMR spectrum of a 0.42 M solution of $(Et_4N)_3[Rh(WS_4)_3]$ collected with a pulse width of 100 μs and a recycle time of 3.78 s. A total of 12 800 transients were collected for this spectrum.

In view of the existence of $M(WS_4)_3^{3-}$ (M = Rh, Ir) it seems that $Pt(WS_4)_3^{2-}$ would be a stable entity. It is known that platinum(IV) can support dianionic sulfur ligands, viz. $Pt(S_5)_3^{2-}$.[24] Our efforts to prepare salts of $Pt(WS_4)_3^{2-}$ focused on the reaction of a

---

[22] Minelli, M.; Enemark, J. H.; Brownlee, R. T. C.; O'Connor, M. J.; Wedd, A. G. *Coord. Chem. Rev.* **1985**, *68*, 169.

[23] For the structure of $Rh(S_2CNEt_2)_3$ see: Raston, C. L.; White, A. H. *J. Chem. Soc., Dalton Trans.* **1975**, 2425.

[24] (a) Wickenden, A. E.; Krause, R. A. *Inorg. Chem.* **1969**, *8*, 779. (b) Spangenberg, M.; Bronger, W. *Z. Naturforsch., B: Anorg. Chem., Org. Chem.* **1978**, *33B*, 482. (c) Recent work: Evans, E. H. M.; Gillard, R. D.; Richards, J. P. G.; Wimmer, F. L. *Nouv. J. Chim.* **1986**, *10*, 783. (d) A recent review: Draganjac, M.; Rauchfuss, T. B. *Angew. Chem., Int. Ed. Engl.* **1985**, *24*, 742.

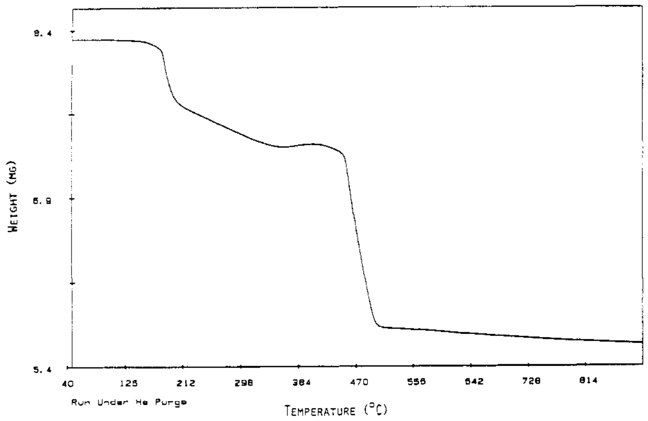

Figure 3. Thermal gravimetric trace for (COD)$PtWS_4$ (carried out under He). Experimental details are given in the Experimental Section.

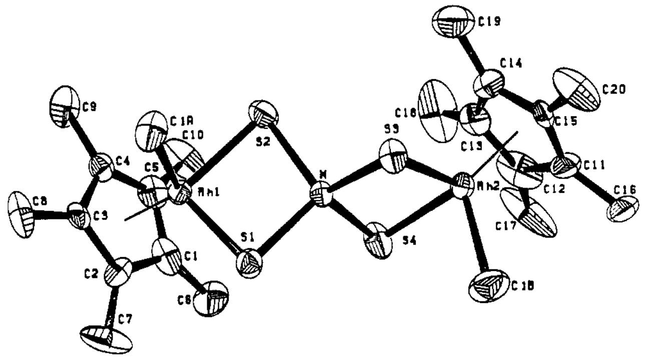

Figure 4. ORTEP plot of $(C_5Me_5)_2Rh_2Cl_2WS_4$ with the thermal ellipsoids drawn at the 35% probability level.

Table I. Thermal Gravimetric Analysis Data

compd	onset temp, °C	final temp, °C	obsd % wt loss	calcd % wt loss	proposed residue formula
$[Rh(COD)]_2WS_4$	230	830	35.89	36.02	($WRh_2S_{2.5}$ or WRh_2S_2O)
$[Rh(COD)]_2MoS_4$	217	830	43.16	43.39	($MoRh_2S_2$)
(COD)$PtWS_4$	195	830	32.88	33.21	(WPtS)
(COD)$PtMoS_4$	180	720	37.79	38.74	(MoPtS)

DMF/acetonitrile suspension of $(Me_4N)_2PtCl_6$[25] with 3 equiv of $(Me_4N)_2WS_4$. From this reaction we obtained a good yield of $(Me_4N)_2[Pt(WS_4)_2]$.[2]

Thermal Gravimetric Studies. As a prelude to a more detailed study, the thermolyses of the cyclooctadiene-containing complexes $[Rh(COD)]_2MS_4$ and (COD)$PtMS_4$ (where M = Mo, W) were examined by thermal gravimetric analysis (TGA). On the basis of the percentage weight loss, the final species have unusual stoichiometries (Table I). Results are shown in Figure 3 for an experiment starting with 8.320 mg of (COD)$PtWS_4$. If only COD were evolved in the first process (≤380 °C), a residual weight of 6.855 mg would be expected whereas the plateau occurs at a somewhat higher weight. The final sloping plateau (≥480 °C) indicates a residual weight consistent with a residue of stoichiometry PtWS. This result was corroborated in a study of (COD)$PtMoS_4$, where the residual weight corresponded to PtMoS (eq 6).

$$(\mathrm{COD})\mathrm{PtMS_4} \xrightarrow{480\ ^\circ\mathrm{C}} \mathrm{PtMS} + 3\mathrm{S} + \mathrm{COD} \qquad (6)$$

Table II. Selected Distances (Å) and Angles (deg) for $(C_5Me_5)_2Rh_2Cl_2WS_4{\cdot}CHCl_3$

W–Rh1	2.908 (2)	W–Rh2	2.892 (2)
Rh1–ClA	2.403 (6)	Rh2–ClB	2.376 (7)
W–S1	2.203 (5)	Rh1–S1	2.401 (5)
W–S2	2.198 (6)	Rh1–S2	2.383 (6)
W–S3	2.187 (6)	Rh2–S3	2.388 (6)
W–S4	2.177 (7)	Rh2–S4	2.381 (6)
Rh1–Cp1[a]	1.79 (2)	Rh2–Cp2[a]	1.79 (3)
Rh1–W–Rh2	167.50 (5)	S1–W–S2	106.2 (2)
S1–W–S3	110.2 (2)	S1–W–S4	111.1 (2)
S2–W–S3	110.8 (2)	S2–W–S4	112.1 (3)
S3–W–S4	106.5 (2)	ClA–Rh1–S1	89.1 (2)
ClA–Rh1–S2	89.4 (2)	ClA–Rh1–Cp1	125.5 (8)
S1–Rh1–S2	94.8 (2)	S1–Rh1–Cp1	123.3 (8)
S2–Rh1–Cp1	124.7 (7)	ClB–Rh2–S3	88.6 (2)
ClB–Rh2–S4	89.3 (3)	ClB–Rh2–Cp2	126.5 (7)
S3–Rh2–S4	94.3 (2)	S3–Rh2–Cp2	123.3 (6)
S4–Rh2–Cp2	124.4 (7)	W–S1–Rh1	78.2 (2)
W–S2–Rh1	78.7 (2)	W–S3–Rh2	78.3 (2)
W–S4–Rh2	78.6 (2)		

[a] Cyclopentadienyl centroid for ring "1" (C1–C5) or ring "2" (C11–C15).

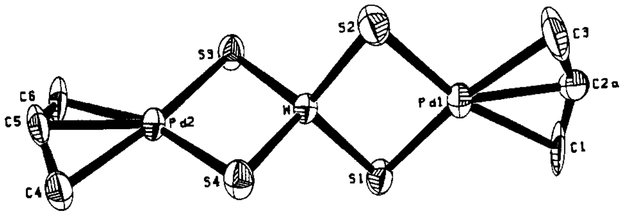

Figure 5. ORTEP diagram of $(allyl)_2Pd_2WS_4$ with thermal ellipsoids drawn at the 35% probability level. The allyl ligand is disordered with respect to C2 (only one of the two disorder positions of C2 is shown). This disorder was satisfactorily described by using a two-position model with occupancy factors of 0.49 and 0.51.

Structure of $[(C_5Me_5)RhCl]_2WS_4$ (4). Compound **4** crystallizes in the unambiguous orthorhombic space group $P2_12_12_1$. The structure (Figure 4) consists of isolated trimetallic units comprised of pseudooctahedral Rh fragments bridged by a tetrahedral WS_4 unit. The coordination sphere of each rhodium consists of a η^5-pentamethylcyclopentadienyl unit, two sulfur atoms, and a chloride ligand. The WS_4 unit is a compressed tetrahedron with two S–W–S angles of 106.2 (2) and 106.5 (2)° while the other S–W–S angles range from 110.2 (2) to 112.1 (3)°; these observed angles are similar to those of $[Rh(COD)]_2WS_4$ (two angles of 105.5 (1) and 106.1 (1)° and the others ranging from 110.8 (1) to 112.4 (1)°). Selected bond distances and angles are presented in Table II. The W–S distances, as we have previously observed, are slightly longer (0.03 Å) than in $(NH_4)_2WS_4$ (2.17 Å (average)).[26] Comparably small increases in the W–S distances of WS_4^{2-} upon complexation to another metal center have been observed; the W–S distances for $[(CuNCS)_2WS_4]^{2-}$ are 2.20 Å (average) while the W–S distances for $[(CuNCS)_4WS_4]^{2-}$ are only slightly longer at 2.23 Å (average).[11a] Similarly, only small increases in the V–S distances are observed in going from $(NH_4)_3VS_4$ to $(Me_4N)_3[VFe_2S_4Cl_4{\cdot}DMF]$.[27] All of the metal–sulfur distances in **4** are slightly longer than those for $[Rh(COD)]_2WS_4$,[1] which contains two d^8 rhodium centers. The W–Rh distances of 2.91 and 2.89 Å are also somewhat longer than those found in $[Rh(COD)]_2WS_4$ (2.87, 2.84 Å). The $Rh–Cl_t$ distances of 2.40 and 2.38 Å are quite similar to those observed for $(C_5Me_5)_2Rh_2Cl_2(\mu\text{-}Cl)_2$.[28]

Structure of $[(allyl)Pd]_2WS_4$ (5). The compound crystallizes in the unambiguous monoclinic space group $P2_1/c$. Four discrete, well-separated molecules occupy the unit cell. The structure consists of a compressed-tetrahedral WS_4 unit with different pairs of sulfur atoms bridging to two palladium atoms (Figure 5). Selected bond distances and angles are presented in Table III. Each palladium atom completes its coordination geometry with an η^3-allyl ligand. The W–S distances (2.21 Å (average)) are similar to those in $[Rh(COD)]_2WS_4$ (2.20 Å (average)[1]) and

---

(25) Jørgensen, C. K. *Acta Chem. Scand.* **1963**, *17*, 1034.

(26) Sasvari, K. *Acta Crystallogr.* **1963**, *36*, 3090.

(27) Do, Y.; Simhon, E. D.; Holm, R. H. *Inorg. Chem.* **1985**, *24*, 4635.

(28) The Rh–Cl(terminal) bond distance is 2.3967 (11) Å; see: Churchill, M. R.; Julis, S. A.; Rotella, F. J. *Inorg. Chem.* **1977**, *16*, 1137.

Table III. Selected Distances (Å) and Angles (deg) for $(allyl)_2Pd_2WS_4$

W–Pd1	2.810 (2)	W–Pd2	2.800 (2)
W–S1	2.216 (6)	Pd1–S1	2.341 (6)
W–S2	2.214 (7)	Pd1–S2	2.343 (7)
W–S3	2.206 (6)	Pd2–S3	2.337 (6)
W–S4	2.211 (6)	Pd2–S4	2.337 (6)
Pd1–C1	2.17 (3)	Pd1–C2A^a	2.14 (5)
C1–C2A^a	1.26 (6)	Pd1–C2B^a	2.12 (5)
C1–C2B^a	1.43 (6)	Pd1–C3	2.16 (4)
C2A^a–C3	1.35 (6)	C2B^a–C3	1.38 (6)
Pd2–C4	2.17 (3)	Pd2–C5	2.09 (3)
C4–C5	1.34 (4)	Pd2–C6	2.16 (3)
C5–C6	1.40 (4)		
Pd1–W–Pd2	177.14 (6)	S1–W–S2	107.9 (2)
S1–W–S3	110.3 (2)	S1–W–S4	110.1 (2)
S2–W–S3	110.2 (2)	S2–W–S4	110.2 (2)
S3–W–S4	108.1 (2)	S1–Pd1–S2	99.8 (2)
S1–Pd1–C1	96.6 (9)	S1–Pd1–C2A	129 (1)
S1–Pd1–C2B	132 (1)	S1–Pd1–C3	165 (1)
S2–Pd1–C1	163.6 (9)	S2–Pd1–C2A	130 (1)
S2–Pd1–C2B	125 (1)	S2–Pd1–C3	94.1 (10)
S3–Pd2–S4	99.8 (2)	S3–Pd2–C4	164.3 (7)
S3–Pd2–C5	131.7 (8)	S3–Pd2–C6	96.6 (7)
S4–Pd2–C4	94.7 (7)	S4–Pd2–C5	126.9 (8)
S4–Pd2–C6	163.1 (7)	W–S1–Pd1	76.1 (2)
W–S2–Pd1	76.1 (2)	W–S3–Pd2	76.0 (2)
W–S4–Pd2	75.9 (2)	C1–C2A–C3	142 (5)
C1–C2B–C3	124 (4)	C4–C5–C6	127 (3)

^{a} Atom C2 disordered.

$[CpRu(MeNC)]_2WS_4$ (2.22 Å (average)[11]) but are longer than in $(NH_4)_2WS_4$ (2.17 Å).[26] The Pd–S distances (2.34 Å (average)) are normal, typical Pd–S distances for thiolate-bridged palladium complexes, for example, 2.31–2.33 Å for $[Pd(t\text{-}BuSCS_2)(t\text{-}BuS)]_2$[29] and 2.31–2.34 Å for $[Pd(SPr^n)_2]_6$.[30] The Pd–C distances of 2.17, 2.09, and 2.16 Å are only 0.03 Å (average) longer than those reported by Oberhansli and Dahl for $(allyl)_2Pd_2Cl_2$.[31] As we have observed in the crystal structure of our other organometallic complexes of tetrathiotungstate, the W–S–Pd angles are acute (76.0° (average)), and the W–Pd distances are relatively short at 2.81 and 2.80 Å. In the lattice, one of the two allyl ligands is disordered with respect to two equivalent positions of the central carbon atom.

Conclusions

In this paper we have surveyed synthetic routes to new types of tetrathiometalate complexes containing rhodium, iridium, palladium, and platinum (Scheme I). Few thiometalate complexes of these metals were known prior to this study, but it appears that there is considerable scope for future work in this area.

Scheme I

$$[Rh(NBD)Cl]_2 + WS_4^{2-} \rightarrow [Rh(NBD)]_2WS_4\ (\mathbf{1})$$

$$[Ir(COD)Cl]_2 + WS_4^{2-} \rightarrow [Ir(COD)]_2WS_4\ (\mathbf{3})$$

$$[(C_5Me_5)RhCl_2]_2 + WS_4^{2-} \rightarrow [(C_5Me_5)RhCl]_2WS_4\ (\mathbf{4})$$

$$[(allyl)PdCl]_2 + WS_4^{2-} \rightarrow [(allyl)Pd]_2WS_4\ (\mathbf{5})$$

$$(COD)PtCl_2 + WS_4^{2-} \rightarrow (COD)PtWS_4\ (\mathbf{7})$$

$$RhCl_3{\cdot}3H_2O + 3WS_4^{2-} \rightarrow Rh(WS_4)_3^{3-}\ (\mathbf{8})$$

One of the unusual features of platinum thiometalates is the availability of complexes with the same metal in both the d^6 and d^8 configurations. Although not demonstrated in this work, the possibility exists that the d^8 complexes could undergo oxidative additions to give d^6 derivatives. Two previously reported examples of octahedral d^6 thiometalate complexes are $Ru(bpy)_2(MoS_4)$ and $FeL_2(WS_4)_2^{2-}$ (L = DMF, pyridine).[7,8]

Our work shows that organic ligands, e.g. olefins, allyl, cyclopentadienyl, are compatible with the presence of the thiometalate coligands. Indeed, the organometallic complexes are the most easily synthesized members of the platinum thiometalates. In the case of the diene complexes, the organic ligands can be easily displaced by good donor ligands such as phosphines and isocyanides. Although organometallic derivatives of the tetrathiometalates may be of interest from the perspective of homogeneous catalysis, the implications for material synthesis also merit attention. Our thermal gravimetric data indicate that the diene complexes can serve as low-temperature precursors to new ternary sulfides. This aspect is the subject of ongoing research in this laboratory, but we note that thiometalates have previously received attention as precursors to inorganic solids such as the 1-D compounds $(NH_4)CuMoS_4$,[12] $MoS(S_2)$,[32] and, more recently, Chevrel phases.[33]

Lastly, the $M(WS_4)_3^{3-}$ ions are noteworthy as a completely new structural class of thiometalate clusters. In principle, these compounds are resolvable into enantiomers and can themselves function as ligands.[34] These compounds do appear to slowly react with electrophilic species such as $[Rh(COD)Cl]_2$; however, this effort has been hampered by solubility problems.

Experimental Section

Materials and Methods. All compounds described herein appear air-stable however, reactions were routinely carried out under a nitrogen atmosphere. Acetonitrile was distilled from calcium hydride under N_2. Methylene chloride was distilled from P_4O_{10} under N_2. All other solvents were reagent grade and were used without further purification. $[Rh(COD)]_2WS_4$,[1] $[Rh(NBD)Cl]_2$,[14] $[Ir(COD)Cl]_2$,[35] $(COD)PtCl_2$,[19] $(\eta^5\text{-}C_5Me_5)_2Rh_2Cl_4$,[17] $(\eta^3\text{-}C_3H_5)_2Pd_2Cl_2$,[36] and $(NH_4)_2MS_4$[37] (M = Mo, W) were prepared by literature methods. $(Ph_4P)_2WS_4$ and $(Ph_4P)_2MoS_4$ were prepared by the metathesis of the corresponding ammonium salt with Ph_4PCl in water.[38] $(Et_4N)_2WS_4$ was prepared by the metathesis of $(NH_4)_2WS_4$ with Et_4NCl in CH_3CN.

^1H NMR spectra were recorded on a Varian XL-200 spectrometer using $CDCl_3$ (with 0.03% TMS) solvent and are reported in ppm versus TMS. $^{31}P\{^1H\}$ NMR spectra were recorded on a locally constructed 250-MHz instrument operating at 101.3 MHz. ^{31}P NMR spectra were measured on CH_2Cl_2 solutions with chemical shifts reported in ppm versus an external standard of 85% H_3PO_4. The ^{183}W NMR spectrum was recorded in a 20-mm sample tube with a General Electric GN-300 wide-bore instrument equipped with a low-frequency probe. Chemical shifts are reported as positive values for downfield shifts (higher frequency) relative to an external standard of a 1 M aqueous solution of Na_2WO_4. Infrared spectra were obtained on Nicolet MX-S FT-IR and Perkin-Elmer 1750 FT-IR spectrophotometers. Elemental analyses were performed by the University of Illinois microanalytical laboratory.

$[Rh(NBD)]_2WS_4$ (1). The addition of an acetonitrile solution (15 mL) of $[Rh(NBD)Cl]_2$ (0.155 g, 0.336 mmol) to an acetonitrile solution (25 mL) of 0.333 g (0.336 mmol) of $(Ph_4P)_2WS_4$ resulted in the immediate precipitation of an orange solid. After 18 h, the orange solid was collected by filtration and washed with CH_3CN and pentane. Recrystallization from CH_2Cl_2/CH_3CN gave 0.177 g (75% yield) of red-orange crystals. Anal. Calcd for $C_{14}H_{16}S_4Rh_2W$: C, 23.95; H, 2.30; S, 18.26; Rh, 29.31; W, 26.18. Found: C, 24.24; H, 2.33; S, 18.02; Rh, 29.17; W, 26.12. ^1H NMR: 2.00 (s, 4 H); 3.97 (s, 4 H); 5.24 (m, 8 H). IR (KI): $\nu_{WS} = 456\ cm^{-1}$.

$[Rh(t\text{-}BuNC)_2]_2WS_4$ (2). A 30-mL CH_2Cl_2 solution containing 0.150 g (0.204 mmol) of $[Rh(COD)]_2WS_4$ was treated with 93 μL of *t*-BuNC (0.816 mmol). After 18 h, 15 mL of hexane was added to the red solution and the volume was reduced to 10 mL in vacuo. Addition of 10 mL of pentane precipitated 0.135 g (78%) of red crystals. Anal. Calcd for $C_{20}H_{36}N_4S_4Rh_2W$: C, 28.25; H, 4.27; N, 6.59; S, 15.08. Found: C,

---

(29) Fackler, J. P., Jr.; Zegarski, W. J. *J. Am. Chem. Soc.* **1973**, *95*, 8566.

(30) Kunchur, N. R. *Acta Crystallogr., Sect. B: Struct. Crystallogr. Cryst. Chem.* **1968**, *B24*, 1623; **1971**, *B27*, 2292.

(31) Oberhansli, W. E.; Dahl, L. F. *J. Organomet. Chem.* **1965**, *3*, 43.

(32) Cramer, S. P.; Liang, K. S.; Jacobson, A. J.; Chang, C. H.; Chianelli, R. R. *Inorg. Chem.* **1984**, *23*, 1215. Scott, R. A.; Jacobson, A. J.; Chianelli, R. R.; Pan, W.-H.; Stiefel, E. I.; Hodgson, K. O.; Cramer, S. P. *Inorg. Chem.* **1986**, *25*, 1461.

(33) Nanjundaswamy, K. S.; Vasanthacharya, N. Y.; Gopalakrishnan, J.; Rao, C. N. R. *Inorg. Chem.* **1987**, *26*, 4286.

(34) Howard, K. E.; Rauchfuss, T. B., unpublished results.

(35) Herde, J. L.; Lambert, J. C.; Senoff, C. V. *Inorg. Synth.* **1974**, *15*, 18.

(36) Tatsuno, Y.; Yoshida, T.; Seiotsuka. *Inorg. Synth.* **1979**, *19*, 220.

(37) Pan, W.-H.; Leonowicz, M. E.; Stiefel, E. I. *Inorg. Chem.* **1983**, *22*, 672.

(38) Stremple, P. Ph.D. Dissertation, University of Iowa, 1983.

28.27; H, 4.52; N, 6.22; S, 14.45. ^{1}H NMR: 1.605 (s). IR (KI): ν_{NC} = 2163 cm^{-1}; ν_{WS} = 455 cm^{-1}. IR (CH_2Cl_2): ν_{NC} = 2164 cm^{-1}.

$[Ir(COD)]_2WS_4$ (3). $[Ir(COD)Cl]_2$ (0.300 g, 0.45 mmol) was dissolved in a minimum of CH_3CN, and this solution was added to a CH_3CN solution (40 mL) containing 0.442 g (0.45 mmol) of $(Ph_4P)_2WS_4$. After the mixture was stirred overnight, the resulting dark orange precipitate was collected by filtration and washed with CH_3CN and pentane. Recrystallization from CH_2Cl_2/CH_3CN gave 0.300 g (74%) of dark brick red microcrystals. Anal. Calcd for $C_{16}H_{24}S_4WIr_2$: C, 21.05; H, 2.65; S, 14.05; Ir, 42.11. Found: C, 21.14; H, 2.69; S, 13.85; Ir, 41.87. ^{1}H NMR: 5.47 (m, 8 H); 2.45 (m, 16 H). IR (KI): ν_{WS} = 464 cm^{-1}.

$[(\eta^5\text{-}C_5Me_5)RhCl]_2WS_4$ (4). A solution of $(Ph_4P)_2WS_4$ (0.495 g, 0.50 mmol) and $(C_5Me_5)_2Rh_2Cl_4$ (0.309 g, 0.50 mmol) in 40 mL of CH_3CN was stirred overnight. The red solution was concentrated and the red microcrystalline product collected and washed with a small amount of CH_3CN followed by pentane. Recrystallization from $CHCl_3/Et_2O$ gave 0.304 g (71%) of red crystals of $(\eta^5\text{-}C_5Me_5)_2Rh_2Cl_2WS_4\cdot CHCl_3$. Anal. Calcd for $C_{21}H_{31}S_4Cl_5Rh_2W$: C, 25.77; H, 3.19; S, 13.11; Cl, 18.11. Found: C, 25.41; H, 2.89; S, 12.70; Cl, 18.66. ^{1}H NMR: 1.97 (s). IR (KI): ν_{WS} = 456 cm^{-1}.

$[(\eta^3\text{-}C_3H_5)Pd]_2WS_4$ (5). Addition of an CH_3CN solution (40 mL) containing 0.183 g (0.50 mmol) of $(allyl)_2Pd_2Cl_2$ to a CH_3CN solution (35 mL) of $(Ph_4P)_2WS_4$ (0.496 g, 0.50 mmol) resulted in the immediate precipitation of a brown solid. After 18 h, the precipitate was collected by filtration and washed with CH_3CN followed by pentane. After it was dried briefly, the solid was extracted into CH_2Cl_2. The CH_2Cl_2 extract was filtered to remove CH_2Cl_2-insoluble material, concentrated, and diluted with hexane. Filtration gave 0.180 g (60%) of golden brown crystals. Anal. Calcd for $C_6H_{10}S_4Pd_2W$: C, 11.87; H, 1.66; Pd, 35.06. Found: C, 12.02; H, 1.66; Pd, 34.99. ^{1}H NMR: 6.03 (septet, 2 H); 5.66 (d, 4 H); 3.97 (d, 4 H). IR (KI): ν_{WS} = 454 cm^{-1}.

(COD)PtMoS$_4$ (6). A solution of 0.965 g (1.069 mmol) of $(Ph_4P)_2MoS_4$ in 50 mL of CH_3CN was added to a solution of 0.400 g (1.069 mmol) of $(COD)PtCl_2$ in 30 mL of the same solvent. A pale brick red precipitate formed upon addition of the MoS_4^{2-} solution. The product was isolated by filtration after 48 h. The isolated material was washed thoroughly with copious amounts of CH_3CN and dried in vacuo. The compound is insoluble in common organic solvents. The yield is 0.525 g (93%). Anal. Calcd for $C_8H_{12}S_4PtMo$: C, 18.22; H, 2.29. Found: C, 18.54; H, 2.17. IR (KI): ν_{WS} = 506, 468 cm^{-1}.

(COD)PtWS$_4$ (7). This compound was obtained in 79% yield analogously to **6**. Anal. Calcd for $C_8H_{12}S_4PtW$: C, 15.61; H, 1.97; S, 20.84. Found: C, 16.17; H, 1.98; S, 20.20. IR (KI): ν_{WS} = 499, 453 cm^{-1}.

$(Ph_3P)_2PtWS_4$. A 60-mL CH_2Cl_2 suspension of $(COD)PtWS_4$ (0.200 g, 0.325 mmol) was treated with a 10-fold excess of triphenylphosphine. After 48 h an orange solution with a small amount of yellow-orange solid was obtained. The reaction mixture was filtered, diluted with hexane, and concentrated to induce precipitation. The product was recrystallized from CH_2Cl_2/hexane to give 0.250 g (75% yield) of yellow microcrystals. ^{31}P NMR: 13.5 (s), $J(^{31}P,^{195}Pt)$ = 3484 Hz. The analogous MoS_4 derivative was prepared in 65% yield. ^{31}P NMR of $(Ph_3P)_2PtMoS_4$: 16.1 (s), $J(^{31}P,^{195}Pt)$ = 3434 Hz.

$(Et_4N)_2[Pt(WS_4)_2]$ from 7. A 10-mL CH_3CN slurry of 0.30 g (0.049 mmol) of $(COD)PtWS_4$ was reacted with a 10-mL CH_3CN solution of $(Et_4N)_2WS_4$ (0.028 g, 0.049 mmol). The yellow slurry becomes a red-orange solution over a period of ca. 2 h. A UV–vis spectrum of the solution (λ_{max} = 410 nm) is identical with that of a solution of independently prepared $(Et_4N)_2[Pt(WS_4)_2]$ of comparable concentration.

$(Et_4N)_3[Rh(WS_4)_3]$ (8). $RhCl_3\cdot 3H_2O$ (0.200 g, 0.76 mmol) and 1.305 g (2.28 mmol) of $(Et_4N)_2WS_4$ in a MeOH/EtOH (300 mL/50 mL) mixture was stirred for 3 days. The brown precipitate was collected by filtration and washed well with MeOH, EtOH, and Et_2O. Recrystallization from CH_3CN/EtOH gave 0.860 g (79%) of brown microcrystals. Anal. Calcd for $C_{24}H_{60}N_3S_{12}RhW_3$: C, 20.16; H, 4.23; N, 2.94; S, 26.91; Rh, 7.20; W, 38.57. Found: C, 19.11; H, 4.12; N, 2.84; S, 25.60; Rh, 6.74; W, 37.60. IR (KI): ν_{WS} = 486, 440 cm^{-1}. UV–vis (CH_3CN solution): 409 nm (10600 M^{-1} cm^{-1}), 378 nm (5400 M^{-1} cm^{-1}). ^{183}W NMR (DMF, acetone-D_6 lock solvent): +2948.0, $J(^{183}W,^{103}Rh)$ = 4.8 Hz. Attempts to grow X-ray-quality single crystals of this compound from DMF/Et_2O or CH_3CN/Et_2O were unsuccessful.

$(Et_4N)_3[Ir(WS_4)_3]$ (9). In a synthesis modeled after that of **8**, 3 equiv of $(Et_4N)_2WS_4$ was reacted with $IrCl_3\cdot 3H_2O$ in a MeOH/EtOH mixture (5:1). From a workup analogous to that in **8**, the compound was obtained in 30% yield. The compound obtained was slightly lighter brown than **8** and was also less soluble in CH_3CN. Anal. Calcd for $C_{24}H_{60}N_3S_{12}W_3Ir$: C, 18.97; H, 3.98; N, 2.77. Found: C, 18.07; H, 3.74; N, 2.81. IR (KI): ν_{WS} = 496, 447 cm^{-1}.

Thermal Gravimetric Analysis. Thermal gravimetric analyses were performed with a Perkin-Elmer TGA-7 instrument equipped with a Perkin-Elmer Series 7500 computer. The TGA studies were carried out up to 900 °C by using a nitrogen flow-through system. Experiments were repeated with He purge gas, with no significant differences in results. The rate of temperature increase was 10 °C min^{-1} in all cases. The residue obtained in the case of $[Rh(COD)]_2WS_4$ was black and finely crystalline, while a black powder was obtained in the case of (COD)-PtMS$_4$ (M = Mo, W).

Table IV. Concentration-Dependent Solution Conductance Results for Et_4NCl, $(Et_4N)_2WS_4$, and $(Et_4N)_3[Rh(WS_4)_3]$

compd	A^a	Λ_0,^{b} Ω^{-1} cm^2 equiv^{-1}	N^c
Et_4NCl	899.4	214.1	1
$(Et_4N)_2WS_4$	2497.4	338.1	1.33
$(Et_4N)_3[Rh(WS_4)_3]$ (**8**)	5219.5	347.4	1.50

^{a}Onsager constant; slope of Λ_e vs $c^{1/2}$. ^{b}Conductance at infinite dilution. $^c N = \sum(\text{ionic charge})/\sum(\text{number of ions})$.

Table V. Crystal Data for Compounds **4** and **5**

formula	$WPd_2S_4C_6H_{10}$	$WRh_2Cl_5S_4C_{21}H_{31}$
cryst syst	monoclinic	orthorhombic
space group	$P2_1/c$	$P2_12_12_1$
a, Å	9.230 (4)	13.179 (2)
b, Å	9.944 (5)	28.725 (7)
c, Å	14.780 (7)	8.258 (2)
β, deg	103.54 (4)	
V, Å^3	1325 (1)	3126 (2)
Z	4	4
density (calcd, obsd), g cm^{-3}	3.042, >2.8	2.079
crystl dimens, mm	0.1 × 0.2 × 0.2	0.2 × 0.3 × 0.3
diffractometer	Syntex P2$_1$	Syntex P2$_1$
μ, cm^{-1}	120.65	54.80
transmission factor range	0.626–0.139 (numerical)	0.402–0.263 (numerical)
extinction	6.4 (8) × 10^{-8}	not applied
2θ limit, deg (octants)	53.0 ($\pm h,+k,+l$)	52.0 ($+h,+k,+l$)
no. of intens (no. of unique intens, R_i)	3151 (2761, 0.071)	4020 (3518, 0.028)
no. of intens $>2.58\sigma(I)$	1534	2664
R	0.066	0.052
R_w (for $w = I/(\sigma^2(F_o) + pF_o^2)$)	0.079 (p = 0.04)	0.059 (p = 0.02)
max density in ΔF map, e Å^{-3}	3.28 (1 Å from W)	1.75 (<1 Å from Rh)

Concentration-Dependent Solution Conductivity of 8. The solution conductivities of Et_4NCl, $(Et_4N)_2WS_4$, and $(Et_4N)_3[Rh(WS_4)_3]$ (**8**) in acetonitrile were measured by using a Barnstead conductivity bridge, Model PM-70CB. The concentration range was 1 × 10^{-2}–5 × 10^{-5} M. A plot of the equivalent conductance Λ_e (defined as the molar conductance divided by N, where N = total number of charges/total number of charge carriers) versus the square root of the concentration yielded straight-line plots.[39] Slopes, determined by least-squares fits of the data, give A, the Onsager limiting constant (which is dependent on electrolyte), and y intercepts give Λ_0, the conductance at infinite dilution.[40] Experimental results are presented in Table IV.

X-ray Crystallography of 4. A suitable crystal for a structure determination was obtained by layering a $CHCl_3$ solution of **4** with diethyl ether. The transparent, red, prismatic crystal used for data collection had well-developed faces and uniformly extinguished plane-polarized light. No decomposition of the crystal was observed during the collection of data, on the basis of the measurement of three standard reflections per 100 intensities measured. Measurements were performed on a Syntex P2$_1$ automated four-circle diffractometer at 27 °C using graphite-monochromated molybdenum radiation. Data collection information is presented in Table V. The data were corrected for Lorentz and polarization effects, anomalous dispersion effects, and absorption.

Structure Solution and Refinement. The structure was solved by direct methods (SHELXS-86); positions for the tungsten and rhodium atoms were deduced from an E map. Subsequent least-squares difference Fourier calculations revealed the positions for the remaining non-hydrogen atoms.

---

(39) Boggess, R. K.; Zatko, D. A. *J. Chem. Educ.* **1975**, *52*, 649. Coetzee, J. F.; Cunningham, G. P. *J. Am. Chem. Soc.* **1965**, *87*, 2529. Geary, W. J. *Coord. Chem. Rev.* **1971**, *7*, 81.

(40) For examples of the measurement of solution conductivity on similar compounds see: Davison, A.; Howe, D. V.; Shawl, E. T. *Inorg. Chem.* **1967**, *6*, 458 See also ref 2a.

Table VI. Positional Parameters for $(C_5Me_5)_2Rh_2Cl_2WS_4{\cdot}CHCl_3$

	x/a	*y/b*	*z/c*
W	0.92789 (6)	0.65039 (3)	0.7877 (1)
Rh1	0.9896 (1)	0.55777 (6)	0.6850 (2)
Rh2	0.8234 (1)	0.73605 (6)	0.8656 (2)
ClA	1.0801 (6)	0.5380 (2)	0.9280 (7)
ClB	0.9531 (5)	0.7871 (2)	0.774 (1)
ClC	0.8222 (5)	0.9282 (3)	0.286 (1)
ClD	0.9335 (6)	0.8768 (3)	0.5221 (8)
ClE	1.0395 (6)	0.9343 (3)	0.290 (1)
S1	1.0756 (4)	0.6315 (2)	0.6816 (7)
S2	0.8515 (5)	0.5845 (2)	0.8463 (8)
S3	0.9500 (4)	0.6924 (2)	1.0058 (7)
S4	0.8396 (6)	0.6928 (3)	0.6209 (7)
C1	0.951 (2)	0.5569 (9)	0.430 (3)
C2	1.054 (2)	0.5384 (7)	0.451 (2)
C3	1.049 (2)	0.4974 (7)	0.556 (2)
C4	0.946 (2)	0.4899 (7)	0.598 (2)
C5	0.886 (2)	0.5247 (9)	0.519 (3)
C6	0.919 (2)	0.5946 (9)	0.322 (3)
C7	1.151 (2)	0.556 (1)	0.373 (3)
C8	1.140 (2)	0.4694 (10)	0.603 (3)
C9	0.917 (2)	0.4468 (8)	0.686 (3)
C10	0.772 (2)	0.526 (1)	0.516 (3)
C11	0.728 (2)	0.7947 (8)	0.944 (3)
C12	0.672 (2)	0.762 (1)	0.812 (4)
C13	0.664 (2)	0.7172 (9)	0.890 (3)
C14	0.710 (2)	0.7213 (9)	1.051 (4)
C15	0.749 (2)	0.7679 (8)	1.077 (3)
C16	0.754 (2)	0.8455 (9)	0.921 (4)
C17	0.633 (3)	0.777 (2)	0.658 (3)
C18	0.608 (2)	0.685 (1)	0.805 (5)
C19	0.711 (2)	0.683 (1)	1.170 (4)
C20	0.801 (2)	0.787 (1)	1.232 (3)
C21	0.927 (2)	0.9261 (8)	0.413 (2)

Hydrogen atom contributions were not included in the structure factor calculations. In the final cycle of least-squares calculations all non-hydrogen atomic positions were refined with anisotropic thermal coefficients. The highest peaks in the final difference Fourier map were located in the vicinity of the tungsten and rhodium atoms. A final analysis of variance between observed and calculated structure factors showed a slight dependence on structure factor amplitude and an inverse dependence on sin θ. Fractional coordinates for the non-hydrogen atoms are presented in Table VI.

It should be noted that the C11–C12 bond, 1.62 (4) Å, deviates from the mean of the remaining Cp-ring C–C bonds, 1.44 (3) Å, by more than 4σ. While this result is statistically significant, some of this deviation may be attributed to the distorted thermal coefficients for atom C12.

X-ray Crystallography of 5. A suitable crystal for X-ray crystallography was obtained by layering a CH_2Cl_2 solution of the compound with pentane, under a dinitrogen atmosphere. The yellow-gold, small, columnar crystal used for data collection was observed to uniformly extinguish plane-polarized light. No crystal decomposition was observed to occur on the basis of three standard reflections, which were monitored after every 100 intensity measurements. Data were collected at 26 °C on a Syntex P2$_1$ automated four-circle diffractometer using graphite-monochromated molybdenum radiation. Data collection parameters are presented in Table V. The data were corrected for Lorentz and polarization effects, anomalous dispersion effects, and absorption.

Table VII. Positional Parameters for $(allyl)_2Pd_2WS_4$

	x/a	*y/b*	*z/c*
W	0.1878 (1)	0.21159 (8)	0.05914 (6)
Pd1	0.3902 (2)	0.2004 (2)	–0.0561 (1)
Pd2	–0.0113 (2)	0.2091 (2)	0.1759 (1)
S1	0.1798 (7)	0.0692 (6)	–0.0569 (4)
S2	0.3772 (8)	0.3495 (7)	0.0640 (5)
S3	–0.0226 (7)	0.3250 (6)	0.0371 (4)
S4	0.2183 (7)	0.1017 (6)	0.1921 (4)
C1	0.459 (3)	0.095 (4)	–0.167 (2)
C2A[a]	0.522 (6)	0.208 (5)	–0.158 (4)
C2B[a]	0.580 (6)	0.169 (5)	–0.111 (4)
C3	0.574 (4)	0.304 (4)	–0.093 (3)
C4	–0.066 (3)	0.109 (3)	0.294 (2)
C5	–0.136 (3)	0.226 (3)	0.277 (2)
C6	–0.229 (3)	0.267 (3)	0.193 (2)

[a] Disordered; relative occupancy 0.49 (5) for site "A".

Structure Solution and Refinement. The structure was solved by Patterson methods; the metal atom positions were deduced from a sharpened Patterson map. A weighted difference Fourier synthesis gave positions for the sulfur atoms, and subsequent least-squares–difference Fourier calculations revealed the positions for the carbon atoms. The hydrogen atoms of the allyl ligands were not included in the structure factor calculations. In the final cycle of least squares, all non-hydrogen atoms were refined with anisotropic thermal coefficients. A group isotropic thermal coefficient parameter was varied for the hydrogen atoms. A 2-fold disorder of the central carbon atom of one allyl ligand was readily refined, with occupation values of 0.49 and 0.51 for the two disordered positions. Successful convergence of the least-squares refinement was indicated by the maximum shift/error for the last cycle of 0.02. In the final difference Fourier map, there was no residual electron density above the background and the highest positive peaks were in the vicinity of the metal atoms. A final analysis of variance between observed and calculated structure factors showed no obvious systematic errors. Fractional coordinates for the non-hydrogen atoms are presented in Table VII.

Acknowledgment. This research was supported by the National Science Foundation. Platinum metals were loaned to us from Johnson Matthey Inc.

Supplementary Material Available: Tables of thermal parameters for compounds **4** and **5** (2 pages); tables of structure factors (21 pages). Ordering information is given on any current masthead page.